Carbohydrate Polymers 113 (2014) 67–76

Contents lists available at ScienceDirect

Carbohydrate Polymers

journal homepage: www.elsevier.com/locate/carbpol

Dissolution enthalpies of cellulose in ionic liquids

Helena Parviainen[a], Arno Parviainen[b], Tommi Virtanen[a], Ilkka Kilpeläinen[b], Patrik Ahvenainen[c], Ritva Serimaa[c], Stina Grönqvist[d], Thaddeus Maloney[e], Sirkka Liisa Maunu[a,*]

[a] Laboratory of Polymer Chemistry, Department of Chemistry, P.O. Box 55, FI-00014 University of Helsinki, Finland
[b] Laboratory of Organic Chemistry, Department of Chemistry, P.O. Box 55, FI-00014 University of Helsinki, Finland
[c] Department of Physics, University of Helsinki, P.O. Box 64, FI-00014 University of Helsinki, Finland
[d] VTT Technical Research Centre of Finland, P.O. Box 1000, FI-02044 VTT, Espoo, Finland
[e] Department of Forest Products Technology, School of Chemical Technology, Aalto University, P.O. Box 16300, 00076 Aalto, Finland

ARTICLE INFO

Article history:
Received 16 May 2014
Received in revised form 30 June 2014
Accepted 2 July 2014
Available online 9 July 2014

Keywords:
Ionic liquid
Cellulose
Fibre dissolution
Differential scanning calorimetry

ABSTRACT

In this work, interactions between cellulose and ionic liquids were studied calorimetrically and by optical microscopy. Two novel ionic liquids (1,5-Diazabicyclo[4.3.0]non-5-enium propionate and *N*-methyl-1,5-diazabicyclo[4.3.0]non-5-enium dimethyl phosphate) and 1-ethyl-3-methylimidazolium acetate–water mixtures were used as solvents. Optical microscopy served in finding the extent of dissolution and identifying the dissolution pattern of the cellulose sample. Calorimetric studies identified a peak relating to dissolution of cellulose in solvent. The transition did, however, not indicate complete dissolution, but rather dissolution inside fibre or fibrils. This method was used to study differences between four cellulose samples with different pretreatment or origins.

1. Introduction

Development of novel solvent systems for cellulose dissolution is a popular research topic. Due to strong inter- and intramolecular hydrogen bonding network cellulose does not dissolve in common molecular solvents. The traditional methods to process cellulose to textile fibres – i.e. the Viscose process, utilizing NaOH and CS_2 to dissolve cellulose, and the Lyocell process, using NMMO (*N*-methylmorpholine-*N*-oxide) – are costly, potentially hazardous and are not sustainable (Wang, Gurau, & Rogers, 2012). Ionic liquids (ILs) and aqueous alkali solvent systems are currently being studied for development of novel sustainable processes for cellulose modification and textile fibre production.

Molten salts capable of dissolving cellulose were first reported in 1934 in a patent by Graenacher, where alkyl pyridinium chlorides were used to solubilise cellulose allowing for homogenous modification (Graenacher, 1934). The distinction between molten salts and ionic liquids is that although both are composed of cation–anion pairs ILs have melting points below 100 °C. The cellulose dissolving capability of dialkyl imidazolium based ILs was demonstrated in 2002 by Swatloski, Spear, Holbrey, and Rogers (2002). The best example for dissolving cellulose in this report was 1-butyl-3-methylimidazolium chloride ([bmim]Cl). Fukaya and coworkers reported the first room-temperature ionic liquids (RTILs) that also possess the capability of dissolving cellulose, such as 1-ethyl-3-methylimidazolium formate ([emim][CO_2H]) (Fukaya, Sugimoto, & Ohno, 2006) or 1-ethyl-3-methylimidazolium dimethylphosphate ([emim][Me_2PO_4]) (Fukaya, Hayashi, Wada, & Ohno, 2008). However, 1-ethyl-3-methylimidazolium acetate ([emim][OAc]) has been a 'benchmark' for cellulose processing ILs due to its excellent capability to dissolve cellulose while retaining relatively low viscosity. Recycling and purification of ILs is necessary for possible industrial applications. King, Asikkala, Mutikainen, Järvi, and Kilpeläinen (2011) introduced distillable ionic liquids (DILs) practically demonstrating the distillation of 1,1,3,3-tetramethylguanidinium propionate. However the viscosity of this IL is rather high for wide applications. It has been shown that the DIL 1,5-diazabicyclo[4.3.0]non-5-enium propionate ([DBNH][CO_2Et]) has similar temperature-viscosity correlation as [emim][OAc], which has a major influence on the practical cellulose dissolution capability (Parviainen et al., 2013). As such, ILs derived from alternative heterocycles can offer interesting properties, compared to imidazoliums.

The compact structure of cellulose fibres restricts the accessibility of chemicals on the surface of fibres. To enhance the reactivity of the pulps they are often subjected to various pretreatments

* Corresponding author.
E-mail address: sirkka.maunu@helsinki.fi (S.L. Maunu).

http://dx.doi.org/10.1016/j.carbpol.2014.07.001
0144-8617/

to make them more accessible. Pretreatments aim to weaken or destroy the outermost layer of the native cellulose fibre that is the most difficult part of the fibre to dissolve. Some pretreatments, such as acid hydrolysis, may destroy the fibre structure almost completely.

Rheological studies have been conducted of polysaccharides and ionic liquids, but differential scanning calorimetry (DSC) studies of polysaccharide–IL interactions are less common. While there are no reports highlighting the dissolution process of cellulose in IL-system by DSC, starch–IL interactions have been previously studied (Mateyawa et al., 2013). Starch and cellulose are both polysaccharides composed of anhydroglucose units. In starch, majority of the anhydroglucose units are connected via α(1→4) glycosidic bonds, while in cellulose they are linked with β(1→4) glycosidic bonds. Starch can also have branches linked with α(1→6) bonds. Differences between starch and cellulose come not only from linear and regular structure of cellulose. In wood cellulose pulp, cell wall layers have different properties due different microfibril orientations and possible residual hemicelluloses and lignin. Starch processing for e.g. production of thermoplastic starch is widely studied (Jiménez, Fabra, Talens, & Chiralt, 2012) and solvents used to process cellulose have been studied for dissolution and modification of starch (Wilpiszewska & Spychaj, 2011). Mateyawa et al. (2013) studied phase transitions of starch in [emim][OAc]-water mixtures using DSC. Starch was mixed with solvent and heated from 25 °C to 120 °C, using 5 °C/min heating rate. Pure water or dilute [emim][OAc]-water solution as solvent resulted in gelatinization of starch and endothermic peaks in the DSC trace. High amount of IL or pure IL gave wide exothermic peaks from starch dissolution. Thermal transitions of starch in NMMO–water mixtures have been studied using DSC by Koganti, Mitchell, Ibbett, and Foster (2011). In high NMMO concentrations, dissolution was exothermic, and with high amount of water in the solvent, gelatinization and an endothermic peak were observed. Total dissolution enthalpy was described to consist of heat of melting and heat of mixing. Heat of melting was stated to be endothermic, but heat of mixing was exothermic and therefore the total heat exchange was exothermic.

In this work, the effect of the pretreatment, crystallinity of cellulose and IL-solvent used on the dissolution of cellulose was studied. Dissolution was followed step by step using optical microscope. Based on the obtained results a qualitative analysis of dissolution patterns and solvent properties was made. Thermal transitions relating to dissolution of cellulose was studied using differential scanning calorimetry.

2. Experimental

2.1. Materials

1-Ethyl-3-methylimidazolium acetate ([emim][OAc], >95%) was obtained from BASF. The water content was 0.15 wt% determined by Karl-Fischer titration. 1,5-Diazabicyclo[4.3.0]non-5-ene (DBN) was purchased from Fluorochem Ltd. and trimethyl phosphate (≥99%) from Sigma–Aldrich.

1,5-Diazabicyclo[4.3.0]non-5-enium propionate ([DBNH][CO_2Et]) was prepared as described by Parviainen et al. (2013). *N*-methyl-1,5-diazabicyclo[4.3.0]non-5-enium dimethyl phosphate ([mDBN][Me_2PO_4]) was prepared using a *Syrris*® glass-jacketed reactor. For a 250 g batch of [mDBN][Me_2PO_4] the following method was used: 116.89 ml (0.946 mol) of DBN was charged to the reactor followed by flushing the headspace with argon gas. 110.71 ml (0.946 mol) of trimethyl phosphate was added to the DBN at 60 °C under argon atmosphere, as to keep the temperature below 80 °C during the exothermic reaction. The mixture was then heated to 75 °C where it was kept for one hour and then cooled to room temperature. The product was an oil-like yellow liquid (Fig. 1).

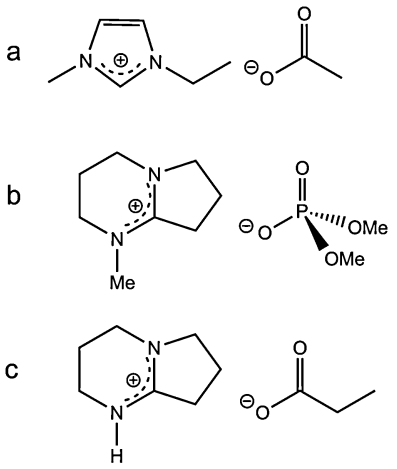

Fig. 1. Chemical structures of ILs used. (a) [emim][OAc], (b) [mDBN][Me_2PO_4] and (c) [DBNH][CO_2Et].

Commercial dried spruce-pine dissolving grade sulphite pulp (cellulose content of 89.9%, viscosity 520 ml/g) from Domsjö Fabriker, Sweden was used in the study. Mechanical and enzymatic pretreatments were carried out at Tampere University of Technology (TUT) and at Finnish Technological Research Center (VTT). The pulp was mechanically shredded with Baker Perkins shredder machine (pulp consistency 20%) for 5 h. This mechanically treated pulp was denoted Pulp1. Enzyme- and mechanically treated pulp was prepared from Pulp1 by enzymatic treatment for 2 h, pH 5, 50 °C, 5% consistency, the enzyme dosage 0.5 mg/g. The enzyme used was a commercial endoglucanase rich enzyme preparation (FiberCare R, Novozym CGP20048). This pulp was denoted Pulp2.

To obtain a low crystallinity pulp, 0.5 g grinding milled (Wiley milled) pulp was weighed. 20 ml 70 wt% aqueous $ZnCl_2$ solution was added while stirring. The mixture was stirred for 2 h. Then the mixture was poured in water. The treated fibres were filtered to remove water and washed carefully. This pulp was denoted Pulp3. The pulp modification procedure was adapted from Mihranyan, Llagostera, Karmhag, Strømme, and Ek (2004).

Food-grade bacterial cellulose (coconut gel in syrup, nata de coco) was homogenized with a blender. To remove sugars, the homogenized gel was dialyzed through a regenerated cellulose tubular membrane (dialysis membrane nominal molecular weight cut-off of 3500 g/mol; Orange Scientific) against distilled water for 4 days. This sample is called nata de coco in this text.

$ZnCl_2$ was purchased from Sigma–Aldrich (purity ≥98%). The water used in the experiments was purified using a Millipore system (UHQ-water). Prior to DSC analysis and optical microscopy, the cellulose samples were freeze-dried.

2.2. Methods

2.2.1. Optical microscopy

Cellulose samples were studied with a polarized light microscope operated with a 10×/0.20 objective (100× magnification). The magnification was the same in all experiments; each picture shown represents 1 mm in height and width. For heating experiments under microscope, Mettler FP 82 hot stage was used to heat the sample between two glass slides. The heating rate was 5 °C/min.

2.2.2. Thermogravimetric analysis

Thermogravimetric analysis (TGA) was performed with Mettler Toledo STAR^e system equipped with a TGA850 thermobalance

using alumina crucibles with lids. The samples were pyrolysed from 25 °C to 600 °C in nitrogen atmosphere. The heating rate was 10 °C/min.

2.2.3. Differential scanning calorimetry (DSC)

TA Q2000 DSC (TA Instruments) was used to study the thermal transitions of cellulose in ionic liquids. 0.75 mg (±0.03 mg) of cellulose was weighed into the 40 μL T_{zero} aluminum pan, ionic liquid was added with a mixing ratio of 1:15 (11.25 mg ± 0.7 mg). After hermetic sealing, the pans were transferred into the DSC instrument for immediate analysis to avoid any time effects. The insertion temperature of the pans was 25 °C. The pans were cooled to 0 °C and then heated to 105 °C at a scanning rate of 5 °C/min. An empty pan was used as a reference. Some heating runs were also conducted using different temperature ranges, mainly from 0 °C to 70 °C to determine the extent of dissolution below 105 °C. The instrument was calibrated using indium as a standard. The Universal Analysis 2000 (TA Instruments–Waters LLC) software was used to analyze the dissolution exotherm (or endotherm) of the DSC traces for the peak temperature (T_{peak}, highest point of the peak, gives the position of the peak in the DSC curve) and the enthalpy (ΔH). Five runs were carried out for each sample to ensure the consistency of the integration results.

2.2.4. NMR analysis of cellulose crystallinity

^{13}C CPMAS NMR measurements were done to obtain the NMR-based crystallinity of cellulose. Crystallinity of cellulose was estimated from the relative areas, obtained by peak-fitting, of the carbon C4 signals for crystalline (92–86 ppm) and non-crystalline (86–80 ppm) cellulose, as described by Virtanen et al. (2014). The spectra were measured with Bruker AVANCE III 500 NMR spectrometer equipped with a double resonance VTN CP-MAS probehead.

2.2.5. X-ray diffraction

Perpendicular transmission geometry was used to measure the crystallinity of the sample with X-ray diffraction. X-rays were generated with a rotating Cu-anode X-ray tube (Rigaku, voltage 50 kV, current 80 mA), monochromatised (Cu $K\alpha_1$, wavelength 0.1541 nm) with a bent Si (1 1 1) crystal and a totally reflecting mirror and imaged with a MAR345 image plate detector (Marresearch, sample-to-detector distance 12 cm). Instrumental broadening and calibration of the scattering angle were determined from the scattering data of silver behenate and lanthanum hexaboride (LaB_6) samples. Data was further corrected for read-out noise, air scattering, polarization, irradiated volume, and detector geometry.

Crystallinity of the sample as measured by X-ray diffraction is the ratio of the crystalline cellulose in the sample to all material in the sample – it is not the same as the cellulose crystallinity determined from NMR measurements. The sample was modelled as a two-component system: an amorphous component (measured sulphate lignin scattering), and the fully crystalline part where either cellulose II (Pulp3) or cellulose Iβ (other samples) diffraction peaks were used in the fitting. A least-squares fit of this model to the corrected experimental data was performed with MATLAB® software. The amorphous contribution was fitted by adjusting the sulphate lignin data multiplying coefficient whereas the crystalline contribution comprised of 17 (Pulp3) or 15 (other samples) strongest diffraction peaks of cellulose.

3. Results

3.1. Pyrolysis of ILs

Pyrolysis of ILs was carried out in order to ensure the thermal stability of the IL-solvents used. Fig. 2 shows TGA scans of the ionic liquids that were used to evaluate the dissolution process of the cellulose samples. [DBNH][CO_2Et] started to pyrolyse around 120 °C and mass loss took place in one step. [emim][OAc] was stable until approximately 100 °C. [mDBN][Me_2PO_4] decomposed more slowly, in two steps. The amount of residue was high at 600 °C, while the other two ILs pyrolysed nearly completely at temperatures well below 300 °C.

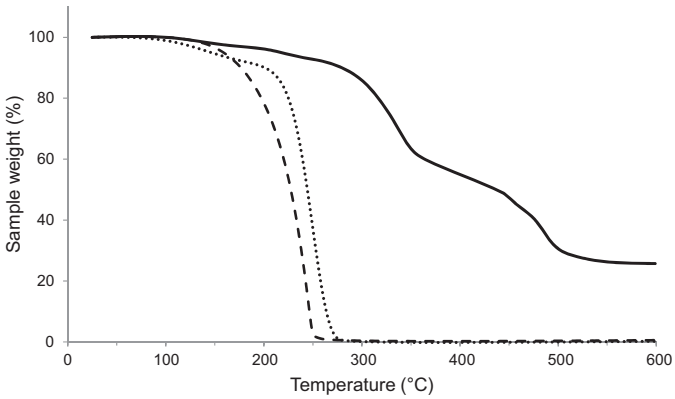

Fig. 2. TGA thermograms of pure ILs. [mDBN][Me_2PO_4]: solid black line, [DBNH][CO_2Et]: dashed line, [emim][OAc]: dotted line.

3.2. Dissolution studies

Dissolution of the samples was followed in three solvents: the two novel ILs ([mDBN][Me_2PO_4] and [DBNH][CO_2Et]) and [emim][OAc] with 10 wt% water. [emim][OAc] was used wet (10 wt% water), because in dry state it dissolves cellulose rather fast even at room temperature (RT), which makes it difficult to follow the dissolution process of fibre wall. Water addition was known to decrease cellulose solubility, but cellulose was still dissolved with heating. All solvents used interact with cellulose even at RT, so observations had to be made immediately after the cellulose and solvent were mixed.

Mechanical shredding was used to break internal bonds within the fibre wall to help fibre swelling. This kind of internal fibrillation allows enzymes to penetrate to the cell wall and cleave cellulose chains. According to the pore size analysis the surface area available to enzymes increases significantly in 5 h of mechanical shredding and is further increased by the action of the enzyme itself (Grönqvist et al., 2014).

The dissolution process was studied using optical microscopy equipped with a hot stage. Micrographs for dissolution of mechanically shredded pulp (Pulp1) in wet [emim][OAc] at 35 °C, 55 °C and 65 °C are shown in Fig. 3a. The both mechanically and enzymatically treated (Pulp2) dissolves in the same solvent by inhomogeneous swelling (results not shown).

Fig. 3b presents the mechanically shredded pulp (Pulp1) heated in [DBNH][CO_2Et] to 35 °C, 65 °C and 75 °C. In this IL the pulp fibres first disintegrate into fragments and then dissolve. The both mechanically and enzymatically treated pulp (Pulp2) dissolves in this IL also with the same mechanism as the only mechanically treated pulp. Fig. 4 presents the structure of the pulp with low crystallinity (Pulp3) and nata de coco, pictured at RT in wet [emim][OAc]. When pulp with low crystallinity (Pulp3) is dissolved in [emim][OAc] with 10 wt% water, the small fragments disappear quickly and the fibres left first swell and then disappear. Nata de coco dissolves without any apparent dissolution mechanisms visible in optical microscopy. The dissolution mechanisms were the same for samples in [mDBN][Me_2PO_4], but required higher temperatures than [emim][OAc] with 10 wt% water for dissolution or

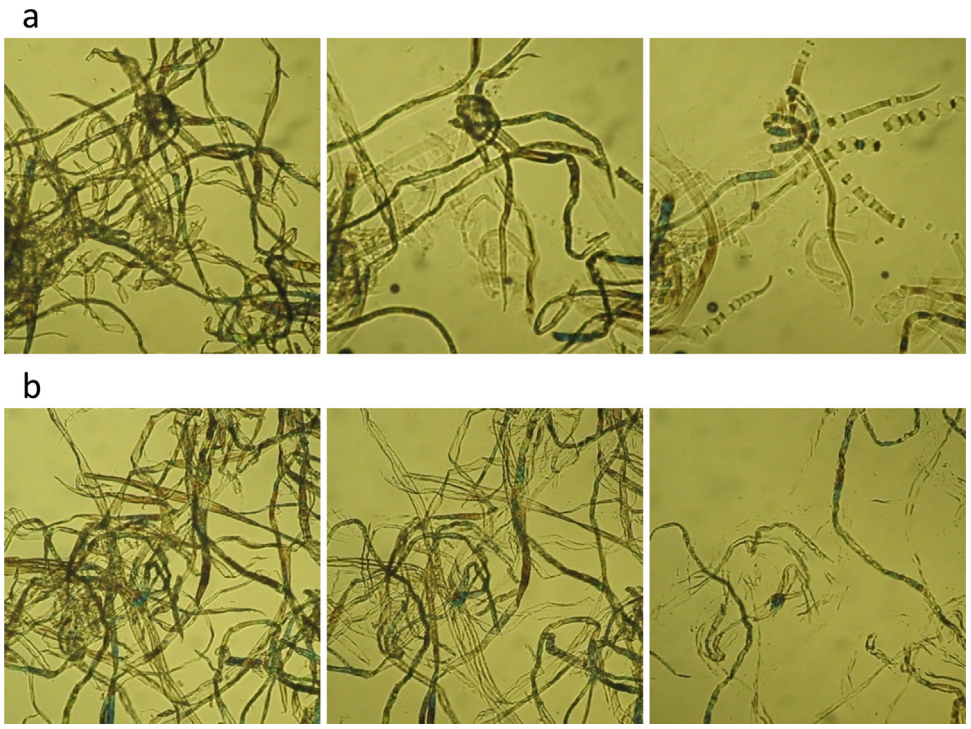

Fig. 3. (a) Pulp1 in [emim][OAc] with 10 wt% water, heated using hot stage. From left: 35 °C, 55 °C and 65 °C. (b) Pulp1 in [DBNH][CO_2Et], heated using hot stage. From left: 35 °C, 65 °C and 75 °C.

swelling to be visible. The black circles seen in some of the pictures are air bubbles.

Dissolution of the samples was also analyzed calorimetrically. The DSC thermograms of cellulose samples dissolving in three solvents are presented in Fig. 5. The samples were heated from 0 °C to 105 °C, 5 °C/min. The characteristic parameters are collected in the Table S1 (supplementary information) and Fig. 7. When pulp fibres were dissolved in the novel ionic liquids an exothermic peak was formed over the temperature range of 40–90 °C, with enthalpies in the range of 90–180 J/g fibre. In [emim][OAc] with 10 wt% water, pulp-based samples showed exothermic peaks in the range of 30–70 °C and enthalpies in the range of 90–110 J/g fibre (Figs. 5 and 7). Heating cellulose samples or ILs alone inside DSC pans did not give any peaks.

In order to see what had happened during dissolution inside the DSC sample pan, sample pans were opened after measurement, the contents were transferred between two glass slides and micrographs were taken. Fig. 6a shows the contents of DSC pans after heating of cellulose in [mDBN][Me_2PO_4] relating the DSC thermograms in Fig. 5a. Undissolved residuals were still visible for all three pulp-based samples after heating to 105 °C in [mDBN][Me_2PO_4]. Pulp-based samples could be fully dissolved in [mDBN][Me_2PO_4], but this required higher temperatures. The microscopy investigation revealed, that dissolution of pulp did not proceed to completion when the sample in [mDBN][Me_2PO_4] was kept at constant 105 °C temperature. Dissolution proceeded when the sample was heated to higher temperature. No additional peaks were seen for heating runs above 105 °C (Fig. S3). When [DBNH][CO_2Et] or [emim][OAc] with 10 wt% water were used and samples were heated up to 105 °C, the amount of undissolved residual was low. Therefore heating runs from 0 °C to 70 °C were conducted. Undissolved outermost fibre walls were seen for mechanically shredded pulp (Pulp1) as well as for both the mechanically and enzymatically treated pulp (Pulp2). Undissolved residuals were seen for the pulp with low crystallinity (Pulp3) (Fig. 6b and c).

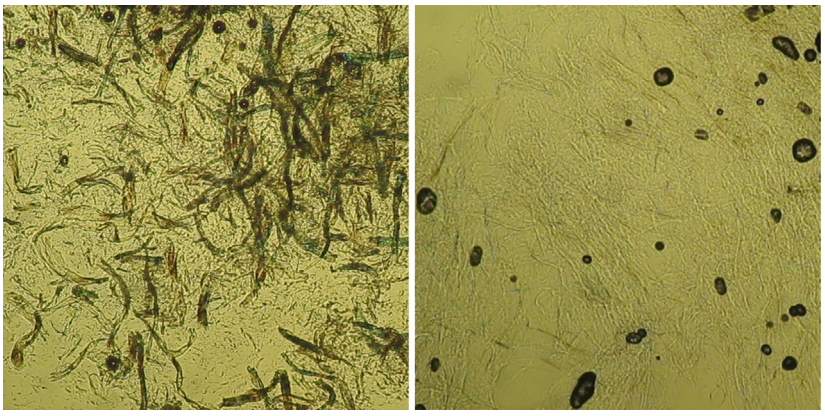

Fig. 4. Pulp3 (left) and nata de coco (right) in wet [emim][OAc] (10 wt% water) at RT.

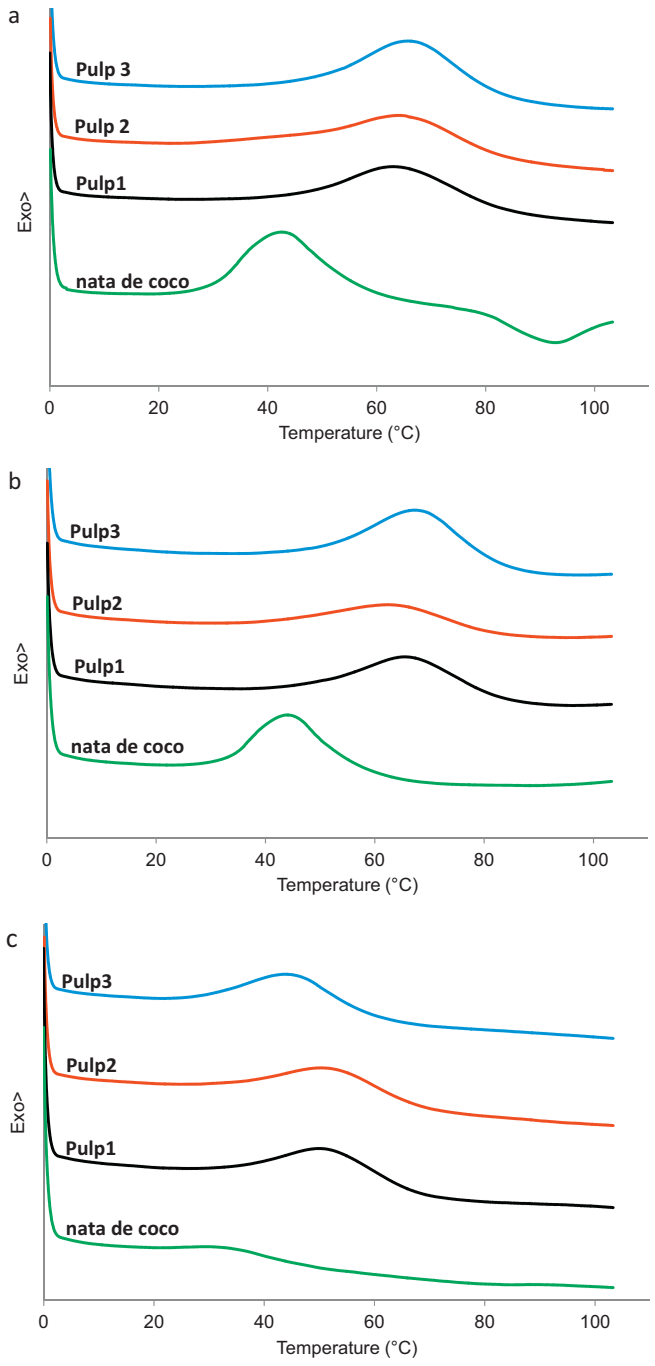

Fig. 5. DSC results for different celluloses in (a) [mDBN][Me_2PO_4], (b) [DBNH][CO_2Et] and (c) wet [emim][OAc] (10 wt% water).

Some cellulose-IL DSC samples were subjected to a sequential heating step. No peaks were detected during the second heating. After the sequential heating (from 0 to 105 °C) in [mDBN][Me_2PO_4], undissolved residuals (although a less amount) were seen for all pulp-based samples.

3.3. Effect of water content in [emim][OAc]

Cellulose dissolution studies with DSC were conducted for water-[emim][OAc] mixtures with increased water contents: 15, 20, 30 and 40 wt% (Fig. 8, parameters in table S2). If the water content of [emim][OAc]-water mixture was increased to 15 wt%, composition known to be a very poor solvent for cellulose, peaks were still seen. Peak temperatures stayed almost the same as with 10 wt% water, even though the ΔH values decreased slightly (Fig. 8). The peak for nata de coco was small already in [emim][OAc] with 10 wt% water (~25 J/g sample) and with 15 wt% water the peak was even smaller (~12 J/g sample) and the sample did not seem to have dissolved when the DSC pan was opened. When sample pans with pulp samples were opened after measurement undissolved residuals, balloons or swollen fibres were seen for all pulp-based samples (Fig. S1, much like in [mDBN][Me_2PO_4] at 105 °C, Fig. 6a).

If the water content was increased to 20 wt%, nata de coco no longer dissolved or showed any peaks. Pulp-based celluloses, however, showed peaks, but T_{peak} and ΔH values were lower. In [emim][OAc] with 20 wt% water, the mechanically shredded (Pulp1) and both mechanically and enzymatically treated pulp (Pulp2) had not dissolved nor significantly swelled and the enthalpies were ca. 40 J/g of fibre. Only the pulp with lower crystallinity (Pulp3) was clearly swollen after the measurement, enthalpy ~67 J/g of fibre.

At 30 wt% water content, the peaks for the mechanically shredded (Pulp1) and both mechanically and enzymatically treated pulp (Pulp2) were almost non-visible (enthalpies <10 J/g fibre) and only the pulp with low crystallinity (Pulp3) showed a clear, although small peak (enthalpy ~23 J/g). When the sample pans were opened after the DSC measurements, microscopy showed that Pulp3 had slightly swollen during heating in [emim][OAc] with 30 wt% water. At 40 wt% water content in [emim][OAc], no peaks or dissolution were seen for any of the samples.

3.4. Crystallinity of studied samples

The crystallinity of the two pretreated softwood dissolving pulps, the low crystalline pulp and the nata de coco were studied in order to obtain information on their structure. Morphological structures were evaluated both using solid state NMR and X-ray diffraction measurements (Table 1).

4. Discussion

Crystallinity of cellulose has been shown to affect cellulose dissolution level for high molecular weight cellulose (Isogai & Atalla, 1991). In the case of pulp fibres this dependence is likely to be obscured by the cell wall structures that slow down the dissolution process. The crystallinity studies carried out here are aimed to clarify the DSC observations. Therefore also nata de coco was studied, even though it certainly has different morphology compared to wood pulps. It was expected also to have the highest crystallinity. There are many studies on methods by which the degree of crystallinity of cellulose is reduced or completely eliminated. These treatments include both milling and chemical methods (Isogai & Atalla, 1998; Mihranyan et al., 2004; Shimura, Nishioka, Kano, Koda, & Nishio, 2014).

Both the cellulose crystallinity and the crystallinity of the sample are the same for Pulp1 and Pulp2 samples within measurement accuracy. The values for crystallinity of the sample determined from X-ray scattering vary based on the analysis method chosen (Park, Baker, Himmel, Parilla, & Johnson, 2010). Most of these methods are intended for relative crystallinity estimation only. The method used in this study, which could be labelled as the amorphous fitting method, gave crystallinity values consistent with NMR determination (Tolonen et al., 2011). This is an interesting observation as mechanically shredded (Pulp1) and both mechanically and enzymatically treated (Pulp2) samples are known to dissolve differently in many solvent systems. The obtained results confirm thus that crystallinity is not the only factor affecting cellulose dissolution.

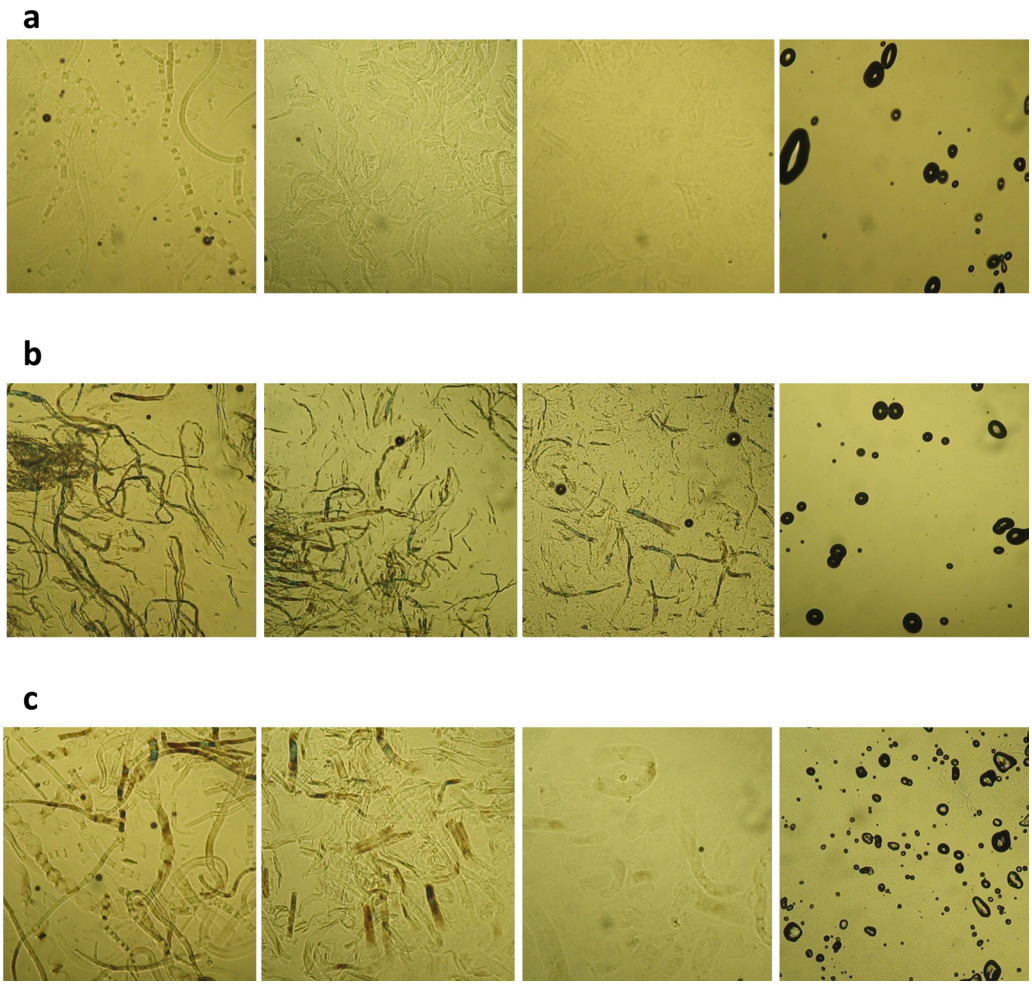

Fig. 6. From left: Pulp1, Pulp2, Pulp3 and nata de coco heated inside DSC sample pan in (a) [mDBN][Me_2PO_4] to 105 °C, (b) [DBNH][CO_2Et] to 70 °C, in which pulp fibres dissolve by disintegrating into fragments, and (c) wet [emim][OAc] (10 wt% water) to 70 °C.

Table 1
Crystallinity of cellulose samples. Standard error for CPMAS crystallinities is estimated to be 3%.

Sample name	Pretreatment	Cellulose crystallinity, CPMAS (%)	Crystallinity of the sample, WAXS (%)
Pulp1	5 h shredding	61	50 ± 5
Pulp2	Enzymatically modified Pulp1	63	53 ± 5
Pulp3	$ZnCl_2$	<20	36 ± 4
Nata de coco	None	78	55 ± 4

The crystalline form present in Pulp3 is mainly cellulose II, which does not show clear separation between crystalline and non-crystalline signals in solid state NMR spectrum. Therefore the cellulose crystallinity given in Table 1 for Pulp3 can be seen as an upper limit. The X-ray scattering intensity of Pulp3 (Fig. S2, supplementary information) showed a clear crystalline contribution which could be fitted with cellulose II diffraction peaks. Although the small crystallite size (approximately 3 nm, see Table S3, supplementary information) results in significant overlap of the contributions of neighbouring crystalline reflections, crystallinity determination is still possible with X-ray scattering.

Both methods yield the highest crystallinity value for the nata de coco sample. The absolute value for cellulose crystallinity obtained with solid state NMR method depends on experimental details, like the contact time used for cross polarization. This value does not depend on the cellulose content of the sample, unlike the X-ray scattering crystallinity.

4.1. Optical microscopy

When cellulose fibres are placed in certain solvents in appropriate temperatures, characteristic inhomogeneous swelling can sometimes be seen. Expanded regions, resembling beads appear along the axis of the fibre while non-swollen sections remain between the beads. These beads are often known as balloons. The ballooning phenomenon of cellulose fibre wall has been studied widely. (Cuissinat & Navard, 2006a, 2006b; Cuissinat, Navard, & Heinze, 2008; Le Moigne, Montes, Pannetier, Höfte, & Navard, 2008; Le Moigne, Bikard, & Navard, 2010; Mangenot, Raison, De Gruy, & Tripp, 1951). When ballooning occurs, the solvent is believed to penetrate inside the fibres through the primary wall. That wall and a part of the secondary wall act as a semi-permeable membrane. The cellulose inside the balloons dissolves before the cellulose of the fibre wall surface layer does. Ballooning of cellulose fibres when dissolved in

aqueous solvents, e.g. NaOH–urea–water, ZnO–NaOH–water and NMMO–water mixtures (Cuissinat & Navard, 2006b) and ionic liquid–cosolvent mixtures, such as [emim][OAc] with 10 wt% water (Olsson, Idström, Nordstierna, & Westman, 2014) as well as in 1-N-butyl-3-methylimidazolium chloride-dimethyl sulfoxide mixture (Cuissinat et al., 2008) has been previously reported. Ballooning can lead to full dissolution or incomplete dissolution, depending on the solvent.

Dissolution of the cellulose samples in ILs was studied using optical microscopy and hot stage. The mechanically shredded pulp (Pulp1) went through ballooning and swelling when heated in [emim][OAc] with 10 wt% water (Fig. 3a) and in [mDBN][Me_2PO_4]. The thinner walled springwood fibres dissolved first and the summerwood fibres were more resistant to dissolution. Ballooning of fibre wall indicates that the outermost fibre wall layers are still at least partially intact and the solvent is not able to directly dissolve these outer layers. The both mechanically and enzymatically treated fibres (Pulp2) dissolved in these solvents by irregular swelling without ballooning due to the missing or damaged outermost cell wall layers, experiencing only irregular swelling. In [DBNH][CO_2Et], the dissolution of both Pulp1 and Pulp2 proceeded by disintegration into fragments (Fig. 3b) and this solvent could be concluded to be a stronger solvent, able to dissolve even the outer fibre wall layers without difficulty. The low crystalline Pulp3 dissolved either by first swelling and then disintegration or just via disintegration, depending on the solvent. Pulp3 had some fibre structures left, but not enough for ballooning (Fig. 4). The structure of nata de coco disappeared without any apparent dissolution mechanisms due to the lack of fibre structure.

Unlike any large-scale dissolution, the dissolution experiments reported/descried here did not involve shear, which is known to be essential for homogeneous solution. Homogeneous IL-cellulose solutions are needed for e.g. modification of cellulose. In this work the dissolution in ILs was used as an analytical method.

4.2. Calorimetric studies

For DSC studies, it is essential that samples are not heated above their decomposition temperature to avoid contamination of the DSC furnace. Therefore the ionic liquids used (Fig. 1) were studied first by thermogravimetric analysis (TGA). All ILs were stable until ~100 °C. The dimethylphosphate anion in [mDBN][Me_2PO_4] is thermally more stable than acetate or propionate, and therefore the amount of pyrolysis residue was high. It should be noted, that the results are comparable for this heating rate (10 °C/min was used) only. As the sample size is known to affect the results, the amounts used were kept as constant as possible. Wendler, Todi, and Meister (2012) studied various imidazole-based ionic liquids using TGA with 20 °C/min heating rate. Their results showed that [emim][OAc] is stable up to 180 °C.

The DSC thermograms of mechanically treated (Pulp1), both mechanically and enzymatically treated (Pulp2), low crystallinity pulp (Pulp3) and nata de coco heated in [mDBN][Me_2PO_4], [DBNH][CO_2Et] and [emim][OAc] with 10 wt% water to 105 °C can be seen in Fig. 5. The positions of the peaks (T_{peak}) and corresponding enthalpies (ΔH) are shown in the Table S1 (supplementary information). Before the detailed discussion of these results it is worthwhile first to clarify, what kind of residuals the samples have left after measurements. Therefore after DSC measurements, sample pans (cooled to RT) were opened and the contents were studied with microscope (Fig. 6). When [DBNH][CO_2Et] or wet [emim][OAc] (10 wt% water) were used as solvents, the amount of visible residuals after heating to 105 °C was low. The pulp-based samples dissolved in [mDBN][Me_2PO_4] had still residues left after heating to 105 °C (Fig. 6a). In order to confirm whether the dissolution mechanism was the same as when the hot stage was used for heating, some heating runs were conducted to only 70 °C. The same ballooning and swelling intermediate stages were seen in wet [emim][OAc] (Fig. 6c) and fragmenting was seen in [DBNH][CO_2Et] (Fig. 6b). These images also revealed the extent of dissolution during the appearance of the peak in DSC thermograms.

Heating a pulp-based sample in [mDBN][Me_2PO_4] to 105 °C does not produce a clear solution. In the pictures of Pulp1, Pulp2 and Pulp3 taken after the heating to 105 °C and cooling to RT, ballooned or swollen fibres are still seen. The amount of swollen fibres was lower in Pulp3 than in Pulp2 (Fig. 6a). Only nata de coco had dissolved into a clear solution. The dissolution mechanism is the same as seen when using optical microscopy and hot stage for heating. Pulps can be fully dissolved to [mDBN][Me_2PO_4], but only by heating to temperature well above 105 °C, at least in the concentration used. No additional peaks were seen when a sample (Pulp1) was heated to 140 °C (Fig. S3). If the heating was stopped to 70 °C, the fibres appeared only swollen, no ballooning had started but the thermogram shows already most of the exotherm. This phase transition has to involve some inner part of the fibre since the outermost layers are still there. Based on this we propose that the enthalpy change in the thermograms involves the dissolution of inner secondary wall cellulose structures. The studies support earlier findings that the recalcitrance of pulp fibres is greatly increased by the presence of the primary and S1 layers on the outer cell wall. In the nata de coco sample where this morphological feature was missing, the dissolution was more complete and occurred at lower temperatures, despite the fact that this sample had the highest crystallinity in the test series. This suggests that the morphology of pulp fibres, especially the organization of microfibrils into layered structures has a dominant effect on cellulose recalcitrance.

When results of DSC curve peak temperatures are compared, differences between pulp-based samples are small. Nata de coco has the lowest peak temperatures. The lower peak temperatures could be argued to be due to the lack of fibre structure in nata de coco. When sample pans were opened after measurements in which the samples were heated to 105 °C, nata de coco had more undissolved residuals in wet [emim][OAc] (10 wt% water) than in novel ILs. On the other hand, the fibre structure of Pulp3 was almost destroyed during the $ZnCl_2$-treatment and this does not affect the peak temperatures so much. When compared to the novel ILs, wet [emim][OAc] gives the lowest peak temperatures for all samples.

The peaks seen in DSC thermograms were integrated. The average values of 5 measurements were calculated (Table S1, Fig. 7). The enthalpy values were normalized to weight of fibres. It should be noted, that the ΔH values are likely to come from several terms. Before measurement, the cellulose and IL are mixed only roughly. The enthalpy of mixing is likely one part of the enthalpy change. Full dissolution and disappearance of the remnant fibre wall structures does not contribute to the ΔH value, seen from the microscopy images compared to DSC thermograms. For the pulp samples no residual slow exothermic process appears after the peak. The transitions appear to have completed. Yet when the sample pans were opened, some amount fibre fragments are observed. This suggests that some regions of the cell wall are highly resistant to dissolution.

Differences in the crystalline structure could have caused some of the differences between samples, not just the amount of crystalline cellulose. Crystallinity does not seem to contribute to the ΔH values, because for the low crystalline sample (Pulp3) the ΔH value does not differ significantly from enthalpy values of Pulp1 and Pulp2. The difference could also be due changes in fibre structure and easier solvent accessibility. The only endotherm observed was for nata de coco between 80 and 100 °C in [mDBN][Me_2PO_4].

Highest ΔH values were obtained for [mDBN][Me_2PO_4]. Error margins were significant for all samples. Concentration differences did not explain the ΔH differences. The solvent was used in excess, in order to ensure proper wetting of cellulose with solvent. The

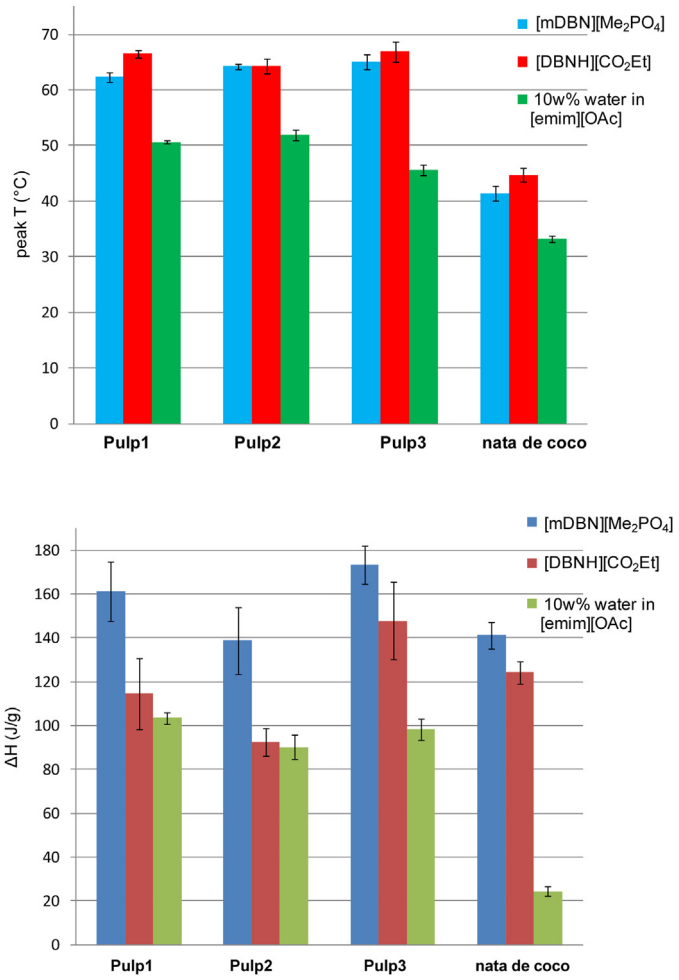

Fig. 7. Diagrams of exotherm T_{peak} and ΔH values for cellulose samples heated in [mDBN][Me_2PO_4], [DBNH][CO_2Et] and [emim][OAc] with 10 wt% water.

concentrations were kept as constant as possible, because the concentration does influence the extent of dissolution or swelling, which can be evaluated visually from Fig. 6. If very high pulp concentration (and low IL amount) was used, some swelling, although not full dissolution took place and exotherms could be seen. When using high cellulose concentrations there is the risk of poor wetting of cellulose, and therefore the enthalpy values would be unreliable. High cellulose concentration would also make it difficult to study the samples with microscopy after DSC measurements. Dissolution mechanism does not seem to determine the ΔH values, since [mDBN][Me_2PO_4] and [emim][OAc] with 10 wt% water dissolve pulps with the same mechanism (Fig. 6a and c, samples heated in DSC and pan opened after cooling to RT), e.g. ballooning of fibre wall if fibres were only mechanically treated, and the ΔH values were very different. The ΔH peaks seem to be an indicator of interaction between solvent and cellulose, but it does not indicate complete dissolution into a homogeneous solution.

Dissolution enthalpies of cellulose have not been widely studied. DSC measurements have been conducted for aqueous alkali systems mainly to determine the interaction of solvent constituents with each other and cellulose in low temperature (Cai & Zhang, 2005; Cai et al., 2007). Isobe et al. (2013) studied the dissolution of microcrystalline cellulose in aqueous LiOH-urea solvent system. Cooling thermograms of pure solvent showed two peaks. Peak at approximately −40 °C was attributed to freezing of LiOH and urea hydrates and peak at −30 °C was ascribed to freezing of bulk water. When cellulose was added to the system, the peak for hydrate freezing decreased or disappeared. A small exotherm was observed between −10 and −15 °C and only in first cooling. This peak was described to be the solvation enthalpy. No integral values were shown for the peaks. Significant cellulose dissolution and swelling is observed in temperatures above this. Ramos, Assaf, El Seoud, and Frollini (2005) studied the dissolution of cellulose in dimethylacetamide/LiCl. In their study the cellulose (microcrystalline cellulose, sisal or cotton linters) and solvent were heated to 150 °C while they were stirred and then allowed to cool after a heating period. During cooling, samples were drawn from the mixture and crystallinities of the samples were determined. The authors calculated the activation enthalpy and entropy form the data of cellulose decrystallization. The enthalpy was negative. Crystallite size and porosity of the cellulose were found to affect the dissolution.

4.3. Water content in [emim][OAc]

There are several reports on effect of water in [emim][OAc] to cellulose dissolution. Olsson et al. (2014) studied dissolution of cellulose in [emim][OAc]-water mixtures, that were stirred for 5 h at 50 °C. 15 wt% water was found to only swell cellulose pulp fibres homogeneously, no balloons were formed. Le, Sescousse, and Budtova (2012) studied dissolution of cellulose in [emim][OAc]-water mixtures. Microcrystalline cellulose (MCC) was stirred at RT for 90 h in various [emim][OAc]-water mixtures. At 15 wt% water, 1 wt% of MCC formed a transparent solution, but 3 wt% MCC showed undissolved crystals. Cellulose was concluded not to be completely dissolved with 15 wt% water in [emim][OAc] and 20 wt% water was found to be the maximal limit for cellulose dissolution. MCC is easier to dissolve than pulp, but also no heating was used, unlike in our study. Phase-diagrams of [emim][OAc]-water and [emim][OAc]-dimethylsulfoxide (DMSO)-binary mixtures were formulated for cellulose (MCC) dissolution (Le, Rudaz, & Budtova, 2014). Solubility was evaluated using optical microscopy. Water was found to compete strongly with cellulose for [emim][OAc], but DMSO was found not to perturb cellulose–IL interactions and allowed the determination of the amount of [emim][OAc] molecules needed to dissolve one anhydroglucose unit of cellulose, this was at least 2.5–3 molecules, independent of DMSO concentration in the [emim][OAc]-DMSO mixture. Froschauer et al. (2013) studied [emim][OAc]-cosolvent mixtures for extraction of hemicelluloses from hemicelluloses-rich paper-grade pulp. Stirring and elevated temperatures (max. 80 °C) were used. Selective dissolution of hemicelluloses was found when paper-grade pulp was stirred in [emim][OAc] with 15–20 wt% water for 3 h at 60 °C. Results from different articles cannot be directly compared, because the type of the cellulose material used, concentration, dissolution temperature and dissolution time affect whether cellulose is dissolved, and not just the water content in [emim][OAc].

Increase of water content in [emim][OAc] from 10 wt% to 15 wt% did not significantly change the peak temperatures of the studied samples although enthalpies decreased somewhat (Fig. 8). Contents of sample pans opened after heating in [emim][OAc] with 15 wt% water showed undissolved residuals, balloons and swollen fibres (Fig. S1, supplementary information). The solvent still dissolved cellulose, but the amount of residuals was high. In [emim][OAc] with 20 wt% or 30 wt% water, only pulp-based samples showed peaks. Possibly the pulp samples have a fraction that dissolved easily, likely due to small particles present in the samples. Pulp3 contains a large amount of tiny debris of cellulose that can swell easily even in very poor solvent. The two other pulp-based celluloses have also some small bits broken off during pretreatment or pulping. The pulp samples are not pure cellulose and the peaks could be an indication of hemicelluloses dissolving. The small peaks can also come from dissolution inside the fibres. Nata de coco is the most pristine sample, not damaged by pulping or pretreatment, and

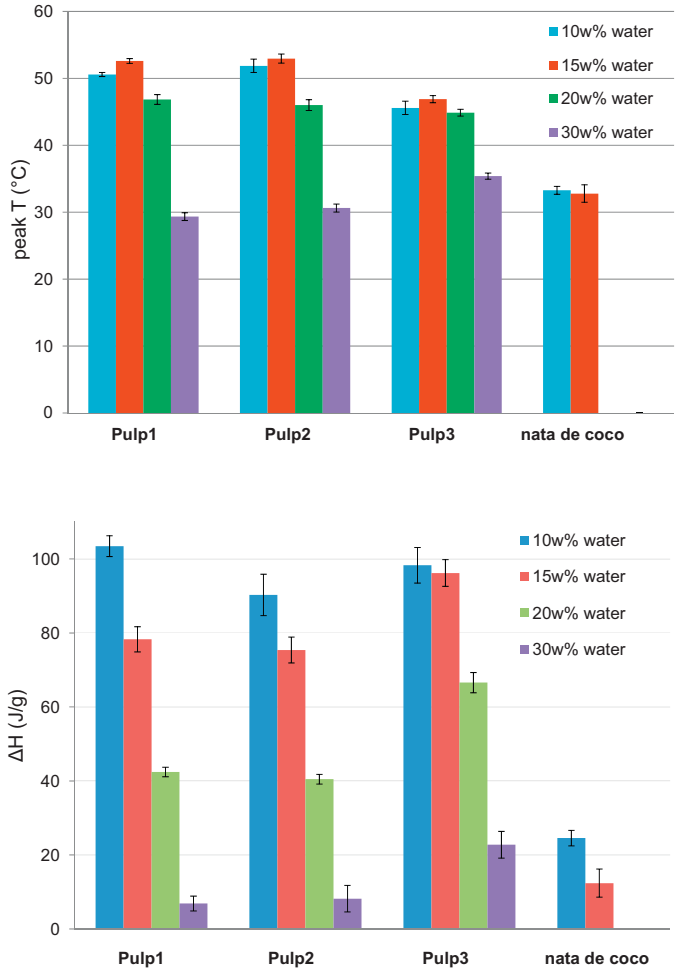

Fig. 8. Diagrams of exotherm T_{peak} and ΔH values for cellulose samples heated in water-[emim][OAc] mixtures. (No peaks or visible dissolution was seen for nata de coco when heated in [emim][OAc] with 20 wt% or 30 wt% water).

possibly therefore does not show any signs of dissolution when heated in very poor solvents, i.e. [emim][OAc] with over 20 wt% water.

5. Conclusions

The dissolution mechanisms of cellulose samples with different pretreatment/origin and crystallinity were investigated using different ionic liquids as solvents. Two softwood dissolving pulps with different pretreatments, mechanical treatment only (Pulp1) and mechanical treatment followed by enzyme treatment (Pulp2), were studied and compared to modified low-crystallinity pulp and bacterial cellulose. Dissolution was followed step by step using optical microscope. Based on the obtained results a qualitative analysis of dissolution patterns and solvent properties was made. Pulp1 and Pulp2 had nearly the same crystallinity, but dissolved differently in some of the solvents used, confirming that crystallinity was not the only factor affecting cellulose dissolution. Further it was studied whether the dissolution process could also be followed calorimetrically. When dissolution of cellulose in ILs was monitored using DSC, exothermic transition was found prior to dissolution (disappearance) of outermost fibre layers. There was no correlation between dissolution mechanisms (ballooning/fragmenting/swelling) and thermal transitions. Appearance of the peak in DSC cannot be seen as an indication of whether a sample has dissolved completely into a homogeneous solution, but rather, that the solvent is able to interact with cellulose in such a way that dissolution/swelling is possible. DSC analysis of dissolution did not allow quantifying the complete dissolution but did give some new information of the complicated dissolution phenomena of cellulose.

Acknowledgements

This work was carried out as a part of the Future Biorefinery Cellulose Program of the Finnish Bioeconomy Cluster (FIBIC). FIBIC and the Finnish Funding Agency for Innovation (TEKES) is acknowledged for its financial support. We thank Marianna Vehviläinen and Taina Kamppuri from TUT for providing the mechanically pretreated pulp and all the other partners for cooperation under this project.

Appendix A. Supplementary data

Supplementary data associated with this article can be found, in the online version, at http://dx.doi.org/10.1016/j.carbpol.2014.07.001.

References

Cai, J., & Zhang, L. (2005). Rapid dissolution of cellulose in LiOH/urea and NaOH/urea aqueous solutions. *Macromolecular Bioscience*, *5*, 539–548.
Cai, J., Zhang, L., Chang, C., Cheng, G., Chen, X., & Chu, B. (2007). Hydrogen-bond-induced inclusion complex in aqueous cellulose/LiOH/urea solution at low temperature. *ChemPhysChem*, *8*, 1572–1579.
Cuissinat, C., & Navard, P. (2006a). Swelling and dissolution of cellulose. Part I. Free floating cotton and wood fibres in N-methylmorpholine-N-oxide–water mixtures. *Macromolecular Symposia*, *244*, 1–18.
Cuissinat, C., & Navard, P. (2006b). Swelling and dissolution of cellulose. Part II. Free floating cotton and wood fibres in NaOH-water-additives systems. *Macromolecular Symposia*, *244*, 19–30.
Cuissinat, C., Navard, P., & Heinze, T. (2008). Swelling and dissolution of cellulose. Part V: Cellulose derivatives fibres in aqueous systems and ionic liquids. *Cellulose*, *15*, 75–80.
Froschauer, C., Hummel, M., Iakovlev, M., Roselli, A., Schottenberger, H., & Sixta, H. (2013). Separation of hemicellulose and cellulose from wood pulp by means of ionic liquid/cosolvent systems. *Biomacromolecules*, *14*, 1741–1750.
Fukaya, Y., Sugimoto, A., & Ohno, H. (2006). Superior solubility of polysaccharides in low viscosity, polar, and halogen-free 1,3-dialkylimidazolium formates. *Biomacromolecules*, *7*, 3295–3297.
Fukaya, Y., Hayashi, K., Wada, M., & Ohno, H. (2008). Cellulose dissolution with polar ionic liquids under mild conditions: Required factors for anions. *Green Chemistry*, *10*, 44–46.
Graenacher, C. US Patent 1943176, 1934.
Grönqvist, S., Hakala, T. K., Kamppuri, T., Vehviläinen, M., Hänninen, T., Liitiä, T., et al. (2014). Fibre porosity development of dissolving pulp during mechanical and enzymatic processing. *Cellulose* [submitted for publication]
Isobe, N., Noguchi, K., Nishiyama, Y., Kimura, S., Wada, M., & Kuga, S. (2013). Role of urea in alkaline dissolution of cellulose. *Cellulose*, *20*, 97–103.
Isogai, A., & Atalla, R. H. (1991). Amorphous cellulose stable in aqueous media: Regeneration from SO_2-amine solvent systems. *Journal of Polymer Science, Part A: Polymer Chemistry*, *29*, 113–119.
Isogai, A., & Atalla, R. H. (1998). Dissolution of cellulose in aqueous NaOH solutions. *Cellulose*, *5*, 309–319.
Jiménez, A., Fabra, M. J., Talens, P., & Chiralt, A. (2012). Edible and biodegradable starch films: A review. *Food and Bioprocess Technology*, *5*, 2058–2076.
King, A. W. T., Asikkala, J., Mutikainen, I., Järvi, P., & Kilpeläinen, I. (2011). Distillable acid–base conjugate ionic liquids for cellulose dissolution and processing. *Angewandte Chemie*, *123*, 6425–6429.
Koganti, N., Mitchell, J. R., Ibbett, R. N., & Foster, T. J. (2011). Solvent effects on starch dissolution and gelatinization. *Biomacromolecules*, *12*, 2888–2893.
Le, K. A., Sescousse, R., & Budtova, T. (2012). Influence of water on cellulose-EMIMAc solution properties: A viscometric study. *Cellulose*, *19*, 45–54.
Le, K. A., Rudaz, C., & Budtova, T. (2014). Phase diagram, solubility limit and hydrodynamic properties of cellulose in binary solvents with ionic liquid. *Carbohydrate Polymers*, *105*, 237–243.
Le Moigne, N., Montes, E., Pannetier, C., Höfte, H., & Navard, P. (2008). Gradient in dissolution capacity of successively deposited cell wall layers in cotton fibres. *Macromolecular Symposia*, *262*, 65–71.
Le Moigne, N., Bikard, J., & Navard, P. (2010). Rotation and contraction of native and regenerated cellulose fibres upon swelling and dissolution: The role of morphological and stress unbalances. *Cellulose*, *17*, 507–519.
Leppänen, K., Andersson, S., Torkkeli, M., Knaapila, M., Kotelnikova, N., & Serimaa, R. (2009). Structure of cellulose and microcrystalline cellulose from various wood species, cotton and flax studied by X-ray scattering. *Cellulose*, *16*(6), 999–1015.

Mangenot, G., Raison, M., De Gruy, I. V., & Tripp, V. W. (1951). Microscopical studies on the swelling of native, bleached and nitrated cellulose fibers. *Botanical Review*, *17*, 555–628.

Mateyawa, S., Xie, D. F., Truss, R. W., Halley, P., Nicholson, T. M., Shamsina, J. L., et al. (2013). Effect of the ionic liquid 1-ethyl-3-methylimidazolium acetate on the phase transition of starch: Dissolution or gelatinization? *Carbohydrate Polymers*, *94*, 520–530.

Mihranyan, A., Llagostera, A. P., Karmhag, R., Strømme, M., & Ek, R. (2004). Moisture sorption by cellulose powders of varying crystallinity. *International Journal of Pharmaceutics*, *269*, 433–442.

Olsson, C., Idström, A., Nordstierna, L., & Westman, G. (2014). Influence of water on swelling and dissolution of cellulose in 1-ethyl-3-methylimidazolium acetate. *Carbohydrate Polymers*, *99*, 438–446.

Park, S., Baker, J. O., Himmel, M. E., Parilla, P. A., & Johnson, D. K. (2010). Cellulose crystallinity index: Measurement techniques and their impact on interpreting cellulase performance. *Biotechnology for Biofuels*, *3*, 10.

Parviainen, A., King, A. W. T., Mutikainen, I., Hummel, M., Selg, C., Hauru, L. K. J., et al. (2013). Predicting cellulose solvating capabilities of acid–base conjugate ionic liquids. *ChemSusChem*, *6*, 2161–2169.

Ramos, L. A., Assaf, J. M., El Seoud, O. A., & Frollini, E. (2005). Influence of the supramolecular structure and physicochemical properties of cellulose on its dissolution in a lithium chloride/*N*,*N*-dimethylacetamide solvent system. *Biomacromolecules*, *6*, 2638–2647.

Swatloski, R. P., Spear, S. K., Holbrey, J. D., & Rogers, R. D. (2002). Dissolution of cellulose with ionic liquids. *Journal of American Chemical Society*, *124*, 4974–4975.

Shimura, R., Nishioka, A., Kano, I., Koda, T., & Nishio, T. (2014). Novel method for producing amorphous cellulose only by milling. *Carbohydrate Polymers*, *102*, 645–648.

Tolonen, L. K., Zuckerstätter, G., Penttilä, P. A., Milacher, W., Habicht, W., Serimaa, R., et al. (2011). Structural changes in microcrystalline cellulose in subcritical water treatment. *Biomacromolecules*, *12*(7), 2544–2551.

Virtanen, T., Penttilä, P., Maloney, T. C., Grönqvist, S., Kamppuri, K., Vehviläinen, M., et al. (2014). Impact of mechanical and enzymatical pretreatments on softwood pulp fiber wall structure studied with NMR spectroscopy and X-ray diffraction. *Cellulose* [submitted for publication].

Wang, H., Gurau, G., & Rogers, R. D. (2012). Ionic liquid processing of cellulose. *Chemical Society Reviews*, *41*, 1519–1537.

Wendler, F., Todi, L.-T., & Meister, F. (2012). Thermostability of imidazolium ionic liquids as direct solvents for cellulose. *Thermochimica Acta*, *528*, 76–84.

Wilpiszewska, K., & Spychaj, T. (2011). Ionic liquids: Media for starch dissolution, plasticization and modification. *Carbohydrate Polymers*, *86*, 424–428.